



Polibits

ISSN: 1870-9044

polibits@nlp.cic.ipn.mx

Instituto Politécnico Nacional

México

Arias, Marvin R.

Analysis of Multipath Propagation based on Cluster Channel Modelling Approach

Polibits, vol. 42, 2010

Instituto Politécnico Nacional

Distrito Federal, México

Available in: <http://www.redalyc.org/articulo.oa?id=402640455009>

- How to cite
- Complete issue
- More information about this article
- Journal's homepage in redalyc.org

redalyc.org

Scientific Information System

Network of Scientific Journals from Latin America, the Caribbean, Spain and Portugal

Non-profit academic project, developed under the open access initiative

# Analysis of Multipath Propagation based on Cluster Channel Modelling Approach

Marvin R. Arias

**Abstract**—The computer simulation approach with an emphasis on the propagation modelling for wireless channels for current and future communication systems is a powerful tool to assess the performance of systems without the need of building them. This paper presents a clustering approach geometry-based channel model, and employs it to derive the power density function (PDF) of the Angle of Arrival (AOA) of the multipath signal components. To evaluate the theoretical clusters PDF in angular domain proposed, we make computer simulations for the geometry-based channel model proposed and compared it with experimental results published in the literature showing good agreement. The clusters PDF derived can be used to simulate the power-delay-angle profile (PDAP) and to quantify second order statistics, i.e., power angular spectrums (PAS) and the associated angular spreads (Ass) for a given elliptical shape of the cluster.

**Index terms**—Angle-of-arrival, angular spread, antenna arrays, channel modelling, clustering, multipath propagation.

## I. INTRODUCTION

RADIO wave propagation in the urban environment is an important issue in the study of wireless communication. In the study of channel propagation, various models, such as empirical models and stochastic modelling based on geometry [1]-[5], is commonly used. In third generation systems like the wideband Code Division Multiple Access (W-CDMA), the physical channel is characterized by multipath propagation. In a scattering environment the propagation paths to a receiving antenna will come from a certain angular spread

Of directions; typically, several versions of the transmitted signal impinge on the receiving antenna from different directions because of multipath. In fact, antenna arrays can be used to implement space-time selective transmission in the downlink and to provide radio localization services. To do so, however, separate knowledge of the directions from which the signals arrive, or angle-of-arrival (AOA), is an important property when characterizing the channel as well as designing receiver algorithms [2]. Since the time and more dominantly the angular spread of the multipath components greatly determines the performance of wireless communication systems. The angular spread essentially determines the diversity gain by using an antenna array [3]. Employing antenna arrays has also been proposed to reduce the co-channel interference by transmitting energy only in the

direction of a specific user and essentially no energy in the directions of other users. The spread is important for diversity schemes and also for determining the AOA. Thus, characterizing the channel in AOA terms is an interesting alternative to standard models. It is now an accepted model that an angular spread occurs from a cluster of scatterers; where the total signal may come from several clusters, see [4]-[8] and referenced there in. As mentioned in [9] a statistical approach is necessary to understand the basic mechanism of propagation.

Several measurement campaigns done in different indoor and outdoor environments, report that multipath components (MPCs) arrive in clusters. Each cluster consists of a group of MPCs with similar angles of arrival (AOAs), angles of departure (AODs), and time of arrival (TOA), corresponding to a dominant path at the receiver (Rx), see [4]-[6], and [9]. Measurements results reported in [4]-[6], and [9], show that the Palladian function is the best fit for estimated AOA in outdoor environments. In this paper, essentially, the main objective is to analytically derive the power density function (PDF) of AOA of the multipath signal for geometry-based statistical channel model that is valid for a circular and elliptical scattering, we assume the double bounce approach channel model as described in [7], [10]. Our contribution would be useful in simulating the power-delay-angle profile (PDAP) and to quantify second order statistics, i.e., angle spread for a given elliptical shape of the cluster of the multipath signal operating in a variety of propagation conditions in urban environment. The propagation environment is composed of scatterers, which are grouped in clusters. Among others, the number of clusters and the average number of scatterers within a cluster can be set with a parameter.

The remainder of the paper is organized as follows. The next section describes the proposed clustering approach channel model and in section 3 based on the channel model proposed, we derive the marginal PDF of the AOA for urban environments. Section 4 presents the simulation results and comparison with experimental results for one typical outdoor scenario in urban environment. Finally, section 5 contains some concluding remarks.

## II. CLUSTERING APPROACH CHANNEL MODEL

This section briefly discussed the clustering approach geometry-based channel model that we use to derive the marginal PDF of the AOA for uniform scatterer density function. We assume that the mobile station (Rx) is stationary or at very low speed and therefore ignore the Doppler effects

Manuscript received May 3, 2010. Manuscript accepted for publication September 10, 2010.

The author is with Department of Electrical Engineering, National University of Engineering, P.O. Box 5595, Managua, Nicaragua (marao@ibw.com.ni).

in the analysis. Since the channel model is geometry-based; (as illustrated in Fig. 1), the signal statistics depend on the position of the base station (Tx) and mobile station (Rx), and the geometrical distribution of the clusters.

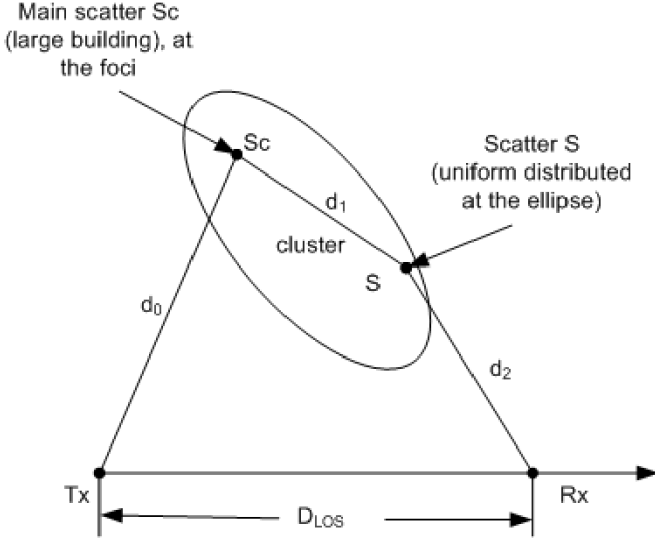


Fig. 1. Geometry-Based clustered multipath propagation model description.

We assume that each cluster (which includes a number of scatterers) is stationary in the far field. We define the angle-delay resolved impulse response of each cluster as [7]

$$h_{(cluster)j}(\tau, \phi) = \sum_{j=1}^J \sum_{i=0}^{L_j} \alpha_{ij} \delta(\phi - \phi_{ij}) \delta(\tau - \tau_0 - \tau_{ij}), \quad (1)$$

where for each cluster:  $|\alpha_{ij}|$  is the magnitude of the scattered source,  $\phi_{ij}$  is the angle-of-arrival of the  $i^{\text{th}}$  multipath component in the  $j^{\text{th}}$  source,  $\tau_0$  represents the extra delay due to the double bounce effect and  $\tau_{ij}$  is the delay associated with that component in the  $j^{\text{th}}$  source. The parameter  $L_j$  is the total number of multipath components associated with the  $j^{\text{th}}$  source. We define the total baseband channel impulse response as follows:

$$h_{total}(\tau, \phi) = \sum_{j=1}^J h_{(cluster)j}(\tau, \phi), \quad (2)$$

The parameter  $J$  is the number of clusters. We analyze for the case of  $J=1$ , i.e., for one cluster condition. From the measurements reported in [4], [6], and [9] the receiver sees six clusters at most in 90% of the cases, thus we use  $J$  as a reference for the parameter, i.e.  $J \leq L$ .

We assume the following restrictions: the cluster region has an elliptical shape because anything outside the ellipse has a large excess delay, i.e., the physical interpretation is that only multipath components with time delay smaller than the specified maximum time delay (bounded by the ellipse), are considered. Therefore, providing that the maximum delay is sufficiently large, nearly all of the power of the multipath signals of a physical channel will be accounted for by the model. The main scatterer ( $Sc$ ), which is a large obstacle far

away from the receiver, (e.g. a large building), is situated at one of the foci of the ellipse as shown in Fig.1. Moreover, there is line of sight (LOS) between the main scatterer and the Rx, and all scatterers ( $S$ ) belonging to the same cluster are uniformly distributed inside it. We further assume that the propagation takes place in the horizontal plane containing the Rx, the Tx and the cluster, which are placed in the same plane.  $D_{LOS}$  represents the Tx-Rx separation distance. In the next section we analyse the approach to derive the marginal PDF of the AOA, using the clustering approach model proposed.

### III. CLUSTER PDF OF ANGLE OF ARRIVAL

Here we present an approach to derive simple general formulas to model the marginal power density function (PDF) of the AOA between the receiver ( $Rx$ ) and the far clusters. Assuming an elliptical shape of the clusters bounded by a circular shape, the approach is described as follows: Firstly in Fig. 2, we describe the details regarding the AOA of the cluster's multipath components (MPCs) at the receiver ( $Rx$ ).

We express the scatterer's density function with respect to the polar coordinates  $(r, \theta)$ , which are related to the rectangular coordinates via the following set of equations:

$$\begin{aligned} r &= \sqrt{x^2 + y^2}, \\ \theta &= \arctan\left(\frac{y}{x}\right), \end{aligned} \quad (3)$$

$$\begin{aligned} x &= r \cos(\theta), \\ y &= r \sin(\theta), \end{aligned}$$

Where  $(x, y)$  denotes the position of the cluster. As shown in Fig. 2, the maximum AOA for the circular case is given by

$$\varphi_{c\max} = \arcsin\left(\frac{a}{R_c}\right), \quad (4)$$

Where " $a$ " is the radius of the circle and  $R_c$  is the distance between the centre of the circle and the Rx. Squeezing in the vertical dimension by a factor  $r_{ab}=b/a$ ,  $0 < r_{ab} \leq 1$  forms the ellipse inside the circle; i.e., the axes of the ellipse produced are major axis  $a = R$  and minor axis  $b = r_{ab} * R$ . From Fig. 2 we can relate the new maximum AOA of the ellipse with the maximum AOA of the circle case by the following expression:

$$r_{ab} \tan(\varphi_{c\max}) = \tan(\varphi_{e\max}), \quad (5)$$

Using (2) and (3) we can obtain a general expression of the maximum AOA for both cases described as follows:

$$\varphi_{e\max} = \arctan\left(r_{ab} \tan\left(\arcsin\left(\frac{a}{R_c}\right)\right)\right), \quad (6)$$

We can note from (4) that it becomes identical to (2) for the particular case of  $r_{ab} = 1$  (Circular case). We also note that the area  $ABCD$  (shaded area within the ellipse in Fig. 2) defined by the x-axis and the line described by points  $ODC$  is in function of the angle  $\phi$ , within the range  $0 < \phi \leq \varphi_{e\max}$ , i.e.,  $A(\phi)$ . Then for a uniform distribution of the scatterers inside

the cluster the cumulative density function (CDF) of the AOA can be defined as follows:

$$F_\varphi(\varphi) = \frac{A(\varphi)}{\frac{1}{2}A_e} = \frac{2A(\varphi)}{ab\pi}, \quad (7)$$

Where  $A_e = ab\pi$  denotes the area of the ellipse. The equation of the ellipse defined in Fig. 2 is

$$\frac{(x-R_c)^2}{a^2} + \frac{y^2}{b^2} = 1, \quad (8)$$

Which we can transform (6) into polar coordinates using and rearranging the relations defined in (1), obtaining a second order equation:

$$r^2 \left( \frac{\cos^2(\varphi)}{a^2} + \frac{\sin^2(\varphi)}{b^2} \right) - r \left( \frac{2R_c \cos(\varphi)}{a^2} \right) + \frac{R_c^2}{a^2} - 1 = 0, \quad (9)$$

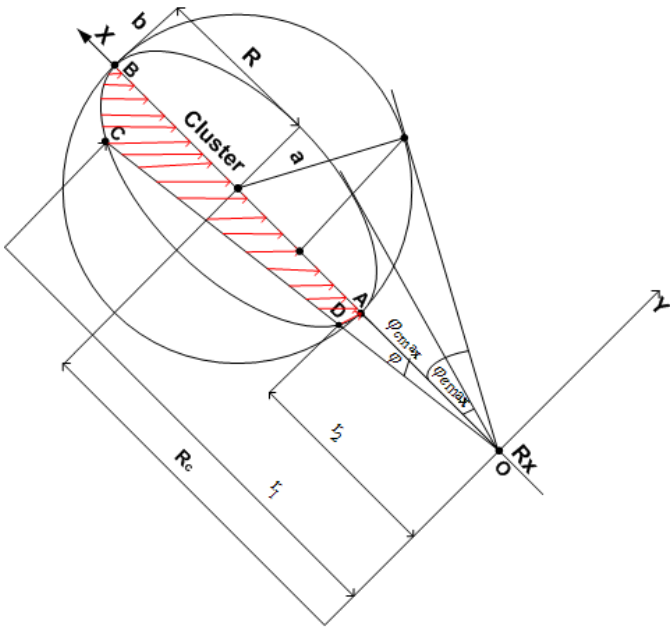


Fig. 2. Geometry of the model for calculating the PDF of the AOA.

Solving (7) with respect to “ $r$ ”, we obtain the following expressions, corresponding to the two radii  $r_1$  and  $r_2$  shown in Fig. 2:

$$r_1 = \frac{R_c b^2 \cos(\varphi) + \sqrt{b^4 a^2 \cos^2(\varphi) - b^2 a^2 \sin^2(\varphi) R_c^2 + b^2 a^4 \sin^2(\varphi)}}{b^2 \cos^2(\varphi) + a^2 \sin^2(\varphi)}, \quad (10)$$

and

$$r_2 = \frac{R_c b^2 \cos(\varphi) - \sqrt{b^4 a^2 \cos^2(\varphi) - b^2 a^2 \sin^2(\varphi) R_c^2 + b^2 a^4 \sin^2(\varphi)}}{b^2 \cos^2(\varphi) + a^2 \sin^2(\varphi)}, \quad (11)$$

An area bounded in function of  $r_1(\varphi)$  and  $r_2(\varphi)$  in polar coordinates is then given by the following expression:

$$A(\varphi) = \frac{1}{2} \int_0^\varphi (r_1^2(\xi) - r_2^2(\xi)) d\xi, \quad (12)$$

Next, inserting (8) and (9) into (10) and the result into (5), we obtain the CDF of the AOA defined by the following integral:

$$F_\varphi(\varphi) = \int_0^\varphi \frac{4bR_c \cos(\xi) \sqrt{-a^2 b^2 (-\cos^2(\xi) b^2 + R_c^2 - R_c^2 \cos^2(\xi) - a^2 + a^2 \cos^2(\xi))}}{a\pi(\cos^2(\xi) b^2 + \sin^2(\varphi) a^2)^2} d\xi, \quad (13)$$

Finally, the PDF of the AOA can be calculated by taking the derivative of the CDF with respect to  $\varphi$ , obtaining the following expression:

$$f_\varphi(\varphi) = \frac{d}{d\varphi} F_\varphi(\varphi) = \begin{cases} \frac{4r_{ab}R_c \cos(\varphi) \sqrt{-a^2 b^2 (-\cos^2(\varphi) b^2 + R_c^2 - R_c^2 \cos^2(\varphi) - a^2 + a^2 \cos^2(\varphi))}}{\pi(\cos^2(\varphi) b^2 + \sin^2(\varphi) a^2)^2}, & \text{for } -\varphi_{\max} < 0 \leq \varphi_{\max} \\ 0, & \text{elsewhere} \end{cases} \quad (14)$$

Since the clusters are bounded by a circle when  $r_{ab} = 1$ ; i.e., for the case  $b=a$ , the AOA of the MPCs (those that make up the same cluster) at the Rx is restricted to an angular region of  $2\varphi_{\max}$ , as illustrated in Fig. 2.

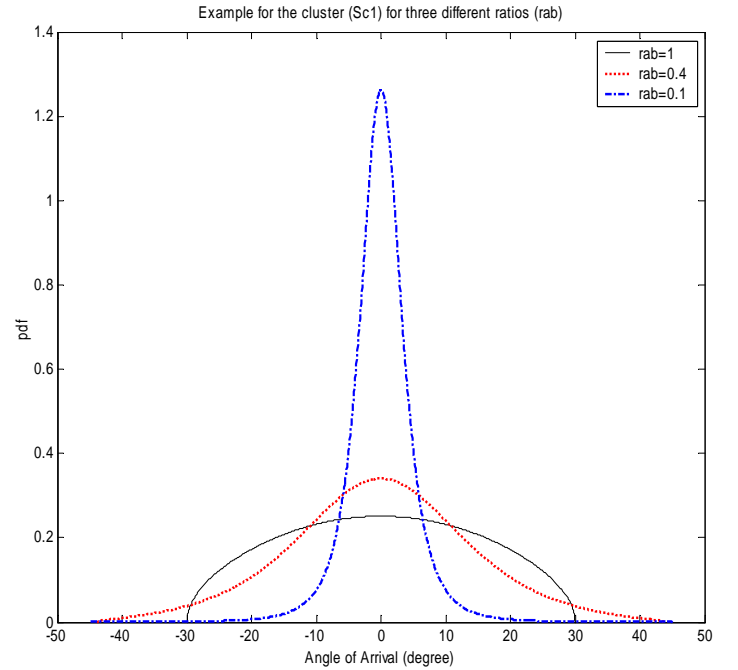


Fig. 3. PDF of AOA for a cluster with three different ratios:  $r_{ab}=1$ ,  $r_{ab}=0.4$ , and  $r_{ab}=0.1$  bounded by a circular cluster, using as a reference the centre of the ellipse as shown in fig.1.

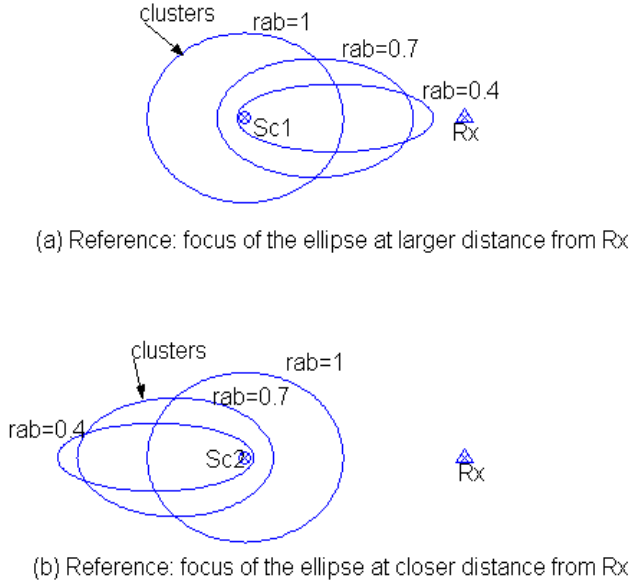


Fig. 4. Area of a cluster with three different ratios:  $r_{ab}=1$ ,  $r_{ab}=0.7$ , and  $r_{ab}=0.4$ . Reference: the separation distances between the cluster (Sc) and the Rx, the foci of the ellipses (a) Sc1 and (b) Sc2, respectively.

Fig. 3 shows one example for the PDF of the AOA, for two different shapes of clusters: for the case of a circular cluster ( $r_{ab}=1$ ), and for two elliptical clusters for the cases  $r_{ab}=0.4$  and  $r_{ab}=0.1$ , respectively. We note from Fig. 2 that the AOA is the maximum for the circular case, as expected from (4) and Fig. 2. For the elliptical cases, we note that the AOA decreases as the ratio  $r_{ab}$  decreases. This is always valid when the circular cluster bounds the ellipses, i.e. when  $r_{ab}=1$ , and the separation distance between the centre of the cluster and the Rx is fixed, as illustrated in Fig. 2.

On the other hand, in our application we consider two cases based on the foci of the ellipses as illustrated in Fig. 4. One case is when we use as a reference for the distance between the Cluster and the Rx the focus of the ellipse (Sc1) situated at larger distance from the Rx as shown in Fig. 4(a). The other case is when we use as a reference the focus of the ellipse (Sc2) situated at closer distance from the Rx as shown in Fig. 4(b).

#### IV. COMPARISON WITH EXPERIMENTAL RESULTS

##### A. Simulation Results

Let us now validate the theoretical pdf using some numerical examples. The theoretical PDF for the AOA described in (12) is evaluated for a test case where the separation distance between the base station as Tx and the mobile unit as Rx is 600 meters, and the assumed separation distance between the cluster and the Rx is 224 meters, which are typical values of distances for outdoors scenarios in urban environments such as City-street scenario or Highway-scenario, see [4], and [11], where the scenarios differ mainly in the size of the environment and the cluster density. The  $(x, y)$  position of two clusters at the same distance from the Rx is

to show the two cases analyzed in the previous section as illustrated in Fig. 5, the results of the power delay angle profiles (PDAPs) obtained from the cluster positions generated are presented in Fig. 6. Note that the AOA is decreasing when we use as a reference the focus of the ellipse situated at closer distance from the receiver as shown previously in Fig. 4(b).

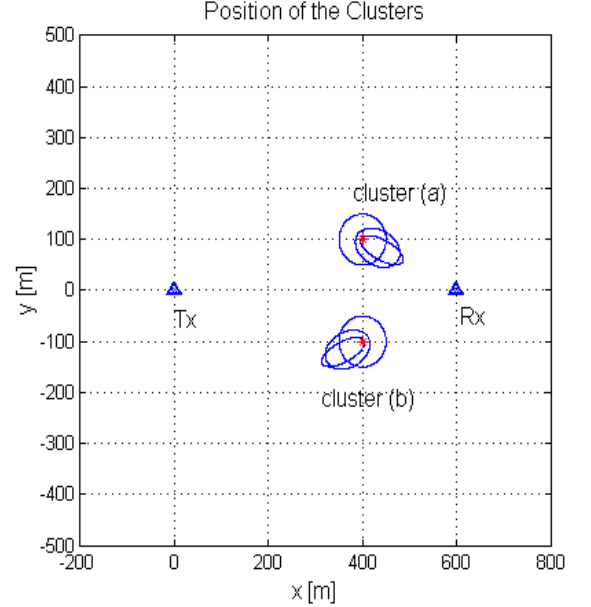


Fig. 5. X-Y Cluster position for three different ratios:  $r_{ab}=0.4$ ,  $r_{ab}=0.7$ , and  $r_{ab}=1$ , respectively.

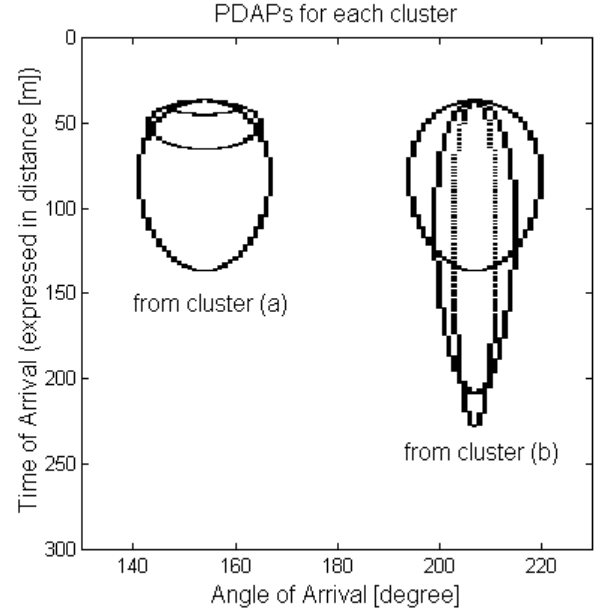


Fig. 6. PDAPs: horizontal axis  $\alpha$ , vertical axis delay expressed in meters, and  $\alpha_{LOS}=180$  deg.

##### B. Comparison with Published Results

Several experimental results are available to which we can compare our theory. In the indoor case, Chong et al. [6] have

characterized the indoor wideband channel model to the angular domain through experimental results obtained by a wideband vector channel sounder together with an eight-element uniform linear array receiver (Rx). MPC parameters were estimated using a super-resolution frequency domain algorithm (FD-SAGE) and clusters were identified in the spatial-temporal domain by a nonparametric density estimation procedure. The clustering effect also gives rise to two classes of channel power density spectra (PDS)-intercluster and intracluster PDS, which are shown to exhibit Laplacian function in the angular domain, such as the power angular spectrums (PASs).

TABLE I  
EXPERIMENTAL RESULTS FROM [4] IN ANGLE (DEGREE.) AND DELAY  
(EXPRESSED IN DISTANCE (M)) OF THE PDAPS  
FOR EACH CLUSTER

Cluster No.	Excess Delay [m]	Delay Spread [m]	Angle-of-arrival $\alpha$ (degrees)	Angle Spread $2\Delta\alpha$ (degrees)
Sc1	150	60	-8	25
Sc2	45	60	-6	6
Sc3	15	60	0	8
Sc4	210	180	0	8

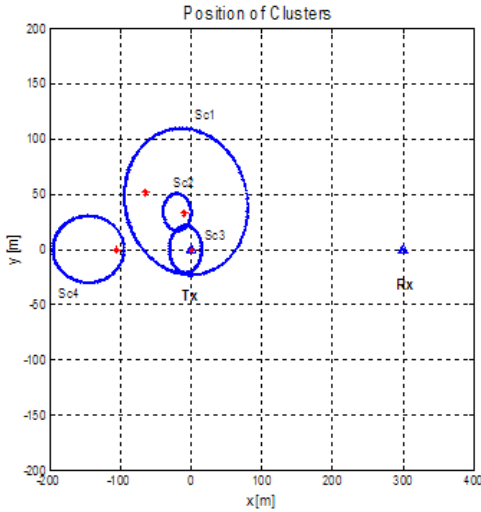


Fig. 7. X-Y Cluster's position obtained, using the experimental results PDAPS from [4] and the double bounce approach as described in [7].

In the outdoor case, Toeltsch et al. [4] used a wideband channel sounder together with a planar antenna array to determine the parameters of the incident waves. A super-resolution algorithm (Unitary ESPRIT) allows resolving individual MPCs in such clusters and hence enables a detailed statistical analysis of the propagation properties. We make comparison with one of the experimental results published in [4], summarized in TABLE I. In this TABLE we present the clusters parameters extracted from the measurement

campaign, i.e., the excess delay, delay spread, (both in terms of distance), AOA, and angle spread, (both in degrees). Then, in Fig. 7 we plotted the position of each cluster based on the measurements of the PDAPS published in [4]. In Fig. 8 we show the boundaries of PDAPS for each cluster obtained from the set of parameters extracted from [4] and defined in TABLE I. As shown in Fig. 7, we can describe different shapes and sizes of clusters found in the PDAPS from measurement campaigns published in the open literature, as in [4].

## V. CONCLUSIONS

This paper presented analytical expressions for the AOA power density function (PDF) and its application in geometrically based channel models using the clustering approach model described in [7].

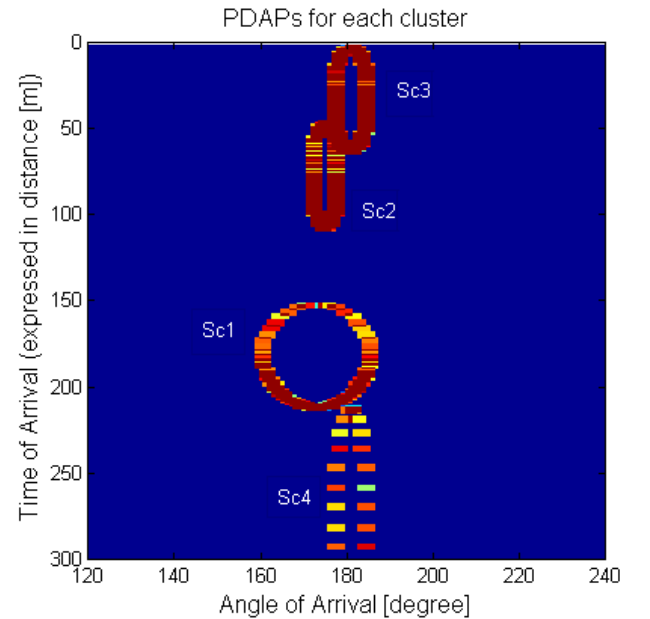


Fig. 8. Boundaries of the PDAPS for each cluster: horizontal axis  $\alpha$ , vertical axis delay expressed in meters, and  $\alpha_{LOS} = 180$  deg.

The average number of clusters and the MPCs distribution within a cluster depend heavily on the resolution of the parameter estimation algorithm. They also depend on the type of scenario, (indoor or outdoor, i.e., the size of the environment and the cluster density). Furthermore, as stated in [6], the number of clusters and MPCs detected also depend on several other factors such as the Tx-Rx separation and location, the physical layout of the environment and the dynamic range of the channel sounder.

## ACKNOWLEDGEMENTS

This work is supported by Swedish International Development Cooperation Agency (SIDCA).

## REFERENCES

- [1] X. Zhao, J. Kivinen, P. Vainikainen, and K. Skog, "Propagation characteristics for wideband outdoor mobile communications at 5.3 GHz," *IEEE J. Select. Areas Commun.*, vol. 20, No. 3, pp. 507-514, Apr. 2002.
- [2] K. I. Pedersen, P. E. Mogensen, and B. H. Fleury, "A stochastic model of the temporal and azimuthal dispersion seen at the base station in outdoor propagation environments," *IEEE Trans. Veh. Technol.*, vol. 49, pp. 437-447, Mar. 2000.
- [3] J. Fuhl, A. F. Molisch, and E. Bonek, "Unified channel model for mobile radio systems with smart antennas," in *Proc. Inst. Elect. Eng.-Radar Sonar Navigation*, vol. 145, Feb. 1998, pp. 32-41.
- [4] M. Toeltsch, J. Laurilla, K. Kalliola, A. F. Molisch, P. Vainikainen, and E. Bonek, "Statistical characterization of urban spatial radio channels," *IEEE Journal on selected areas in Communications*, vol. 20, No. 3, pp. 539-549, April 2002.
- [5] J. P. Kermoal, L. Schumaker, K. I. Pedersen, P. E. Mogensen, and F. Frederiksen, "A stochastic MIMO radio model with experimental validation," *IEEE Journal on selected areas in Communications*, vol. 20, No. 6, pp. 1211-1226, June 2002.
- [6] C. C. Chong, Ch. M. Tan, D. I. Laurenson, and S. McLaughlin, "A New Statistical Wideband Spatio-Temporal Channel Model for 5-GHz Band WLAN Systems," *IEEE Journal on selected areas in Communications*, vol. 21, No. 2, pp. 139-150, February 2003.
- [7] M. R. Arias and B. Mandersson, "Clustering Approach for Geometrically Based Channel Models in Urban Environments," *IEEE Antennas and Wireless Propagation Letters*, vol.5, pp 290-293, December, 2006.
- [8] A. F. Molisch, "A Generic Model for MIMO Wireless Propagation Channels in Macro-and Microcells," *IEEE Transactions on Signal Processing*, vol. 52 No. 1, pp 61-71, January 2004.
- [9] J. B. Andersen and K.I. Pedersen, "Angle-of-Arrival Statistics for Low Resolution Antennas," *IEEE Transactions on Antennas and Propagation*, vol. 50, No. 3, March 2002.
- [10] M. R. Arias and B. Mandersson, "A Generalized Angle Domain Clusters PDF and Its Application in Geometrically Based Channel Models," in *Proc. Fifth International Conference on Information, Communications & Signal Processing, ICICS 2005*, vol.1, December, 2005, pp 1339-1343.
- [11] J. M. Gil, F. C. Cardoso, B. W. Kuipers, and L. M. Correia, "Contribution for the Definition of Common Propagation Scenarios", *IST-NEWCOM Project Report*, Lisbon, Portugal, May 2005.